



Capturing interactions in pedestrian walking behavior in a discrete choice framework

Gianluca Antonini, EPFL

Michel Bierlaire, EPFL

Conference paper STRC 2006

STRC

6th Swiss Transport Research Conference

Monte Verità / Ascona, March 15-17, 2006

Capturing interactions in pedestrian walking behavior in a discrete choice framework

Gianluca Antonini
Signal Processing Institute, EPFL
Lausanne

Phone: +41 21 693 46 20

Email: gianluca.antonini@epfl.ch
February 2006

Michel Bierlaire
Institute of Mathematics, EPFL
Lausanne

Phone: +41 21 693 25 37

Fax: +41 21 693 55 70

Email: michel.bierlaire@epfl.ch

Abstract

In this paper we propose a general framework for pedestrian walking behavior, based on discrete choice modeling. Two main behaviors are identified: *unconstrained* and *constrained*. The constrained patterns are further classified into *attractive interactions* and *repulsive interactions*. The formers are captured by a *leader-follower* model while the latter through a *collision avoidance* model. The spatial correlation between the alternatives is taken into account defining a cross nested logit model. Quantitative analysis is performed by maximum likelihood estimation on a real dataset of pedestrian trajectories, manually tracked from video sequences.

Keywords

Pedestrian behavior – Interactions – Behavior models – STRC 2006 – Monte Verita

1 Introduction

Pedestrian behavior modeling is an important topic in different contexts. Architects are interested in understanding how individuals move into buildings to find out optimality criteria for space design. Transport engineers face the problem of integration of transportation facilities, with particular emphasis on safety issues for pedestrians. Recent tragic events have increased the interest for automatic video surveillance systems, able to monitoring pedestrian flows in public spaces, throwing alarms when abnormal behaviors occur. Special emphasis has been given to more specific evacuation scenarios, for obvious reasons. In this spirit, it is important to define mathematical models based on specific (and context-dependent) behavioral assumptions, tested by means of proper statistical methods. Data collection for pedestrian dynamics is particularly difficult and few models presented in the literature have been calibrated and validated on real datasets.

In this work we refer to the general framework for pedestrian behavior described by Hoogendoorn (in press) and Daamen (2004). Individuals in a certain environment make different decisions, following a hierarchical scheme: *strategical*, *tactical* and *operational*. Briefly, destinations and activities are chosen at a strategical level; the order of the activity execution, the activity area choice and route choice are performed at the tactical level while instantaneous decisions are taken at the operational level. In this paper we address the problem of pedestrian walking behavior, naturally identified by the operational level of the hierarchy just described. We are interested in modeling the short range behavior in *normal* conditions, as a reaction to the surrounding environment and to the presence of other individuals. With the term “normal” we refer to non-evacuation and non-panic situations.

The objective in this paper is to provide a disaggregate, fully estimable behavioral model based on discrete choice analysis, calibrated on real pedestrian trajectories manually tracked from video sequences. We keep the same spatial discretization and choice set definitions introduced in Antonini, Bierlaire, and Weber (to appear) and shortly reviewed later on in this section. Two types of behavior are modeled here: *unconstrained* and *constrained*. The constrained patterns are further classified into *attractive interactions* and *repulsive interactions*. This conceptual framework is illustrated in Figure 1.

The unconstrained decisions are independent from the presence of other pedestrians and are generated by subjective and/or unobserved factors. The first of these factors is represented by the individual’s destination. It is assumed to be exogenous to the model and decided at the strategical level. The second factor is represented by the tendency of people to keep their current direction, minimizing their angular displacement. Finally, unconstrained accelerations (with accelerations we mean both positive and negative speed variations) are dictated by the individual desired speed. The implementation of these ideas is made through the three unconstrained patterns indicated in Figure 1.

The main contribution of this paper consists in a detailed analysis of the constrained behaviors.

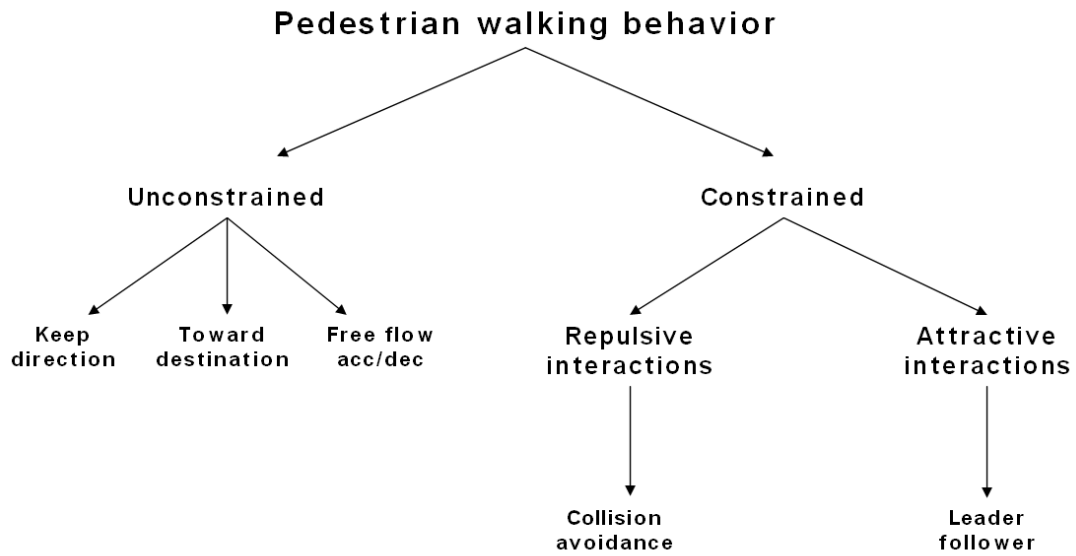


Figure 1: Conceptual framework for pedestrian walking behavior

We assume that behavioral constraints are induced by the interactions with the other individuals in the scene. Repulsive interactions are modeled through the *collision avoidance* pattern, which is designed to capture the effects of possible collisions on the current trajectory of the decision maker. Attractive interactions are modeled through the *leader-follower* behavior, that is the tendency of people to follow another individual in a crowd, in order to benefit from the space she is creating. Here, the existence of one or more leaders is assumed. They are represented by those individuals in a neighbour of the decision maker and with similar moving directions and speed, affecting her decisions.

Previous methods for pedestrian behavior modeling can be classified in two main categories: *microscopic* and *macroscopic* models. In the last years much more attention has been focussed on microscopic modeling, where each pedestrian is modeled as an agent, individually. Examples of microscopic models are the *social forces* model in Helbing and Molnár (1995) and Helbing et al. (2002) where the authors use Newtonian mechanics with a continuous space representation to model long-range interactions. Blue and Adler (2001) and Schadschneider (2002) use cellular automata models, characterized by a static discretization of the space where each cell in the grid is represented by a state variable. Another microscopic approach is based on space syntax theory where people move through spaces following criteria of space visibility and accessibility (see Penn and Turner, 2002) and minimizing angular paths (see Turner, 2001). Finally, Borgers and Timmermans (1986), Whyne et al. (1996) and Dellaert et al. (1998) focus on destination and route choice problems on network topologies. For a general literature review

on pedestrian behavior modeling we refer the interested reader to Bierlaire et al. (2003).

In Antonini et al. (to appear) a discrete choice framework for pedestrian walking behavior is defined, modeling the choice of “where to put the next step” in a microscopic context. Pedestrian movements and interactions take place on the horizontal walking plane. The spatial resolution depends on the current speed vector of the individuals. The geometrical elements of the space model are illustrated in figure 2

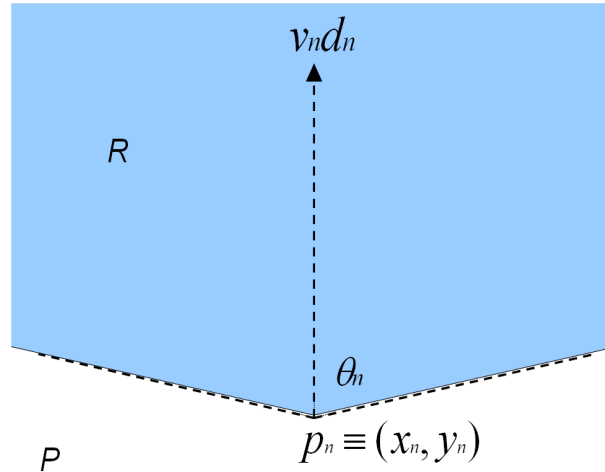


Figure 2: The basic geometrical elements of the space structure

The current position of the decision maker n is p_n , her current speed $v_n \in \mathbb{R}$, her current direction is $d_n \in \mathbb{R}^2$ (normalized, so that $\|d_n\| = 1$) and her visual angle is θ_n . The region of interest is situated in front of the pedestrian, ideally overlapping with her visual field, and is schematically represented by the shaded area in figure 2. An adaptive discretization is obtained assuming three speed regimes, where the individuals can accelerate and decelerate up to a certain factor or they can keep their current speed constant. A choice between 11 radial directions is allowed, as illustrated in Figure 3.

A choice set of 33 alternatives is generated where each alternative corresponds to a speed regime v and a radial direction d . They are numbered using $na = 11s + r$ where na is the number of the alternative, s and r are, respectively, the speed regime and the direction indexes, as reported in Figure 3. Each alternative is identified by the physical center of the corresponding cell in the spatial discretization c_{vd} , that is

$$c_{vd} = p_n + vtd,$$

where t is the time step. The choice set varies with direction and speed therefore the distance between an alternative's center and other pedestrians will vary with the speed of the decision

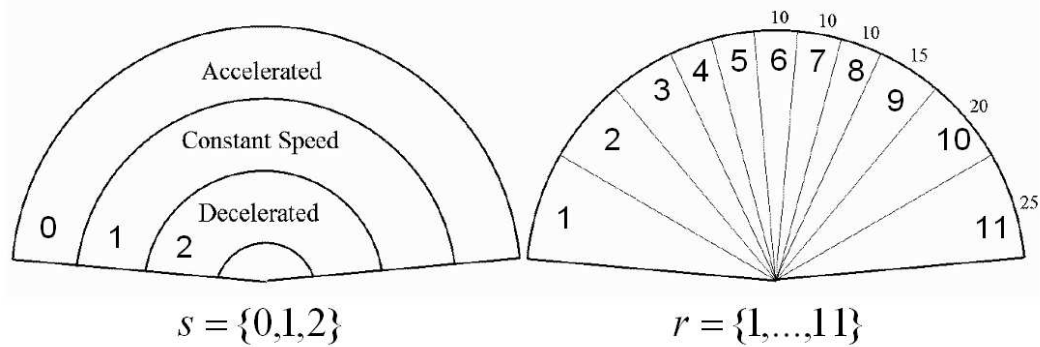


Figure 3: The spatial discretization is generated assuming three speed regimes and 11 radial directions. The external numbers in the right-hand figure represent the angular amplitudes of the radial cones, in degrees. The internal numbers (r) refer to the enumeration of directions while s in the left-hand figure represents the indexes used for speed regimes

maker. As a consequence, differences in individual speeds are naturally mapped into differences in their relative interactions.

The concept of leader-follower has been inspired by previous car following models in transport engineering (Ahmed, 1999; Herman and Rothery, 1965; Lee, 1966; Newell, 1961, among others). The main idea in these models is that two vehicles are involved in a car following situation when a subject vehicle follows a leader, normally represented by the vehicle in front, reacting to its actions. In general, a sensitivity-stimulus framework is adopted. According to this framework a driver reacts to stimuli from the environment, where the stimulus is normally chosen as the leader relative speed. Different models differ in the specification of the sensitivity term. This modeling idea is extended here and adapted to the more complex case of pedestrian behavior. We want to stress the fact that in driver behavior modeling a distinction between acceleration behavior and direction change (lane change) behavior is almost natural (see Toledo, 2003), being imposed by the transport facility itself. On the other hand, the pedestrian case is more complex, the movements being purely two-dimensional on the walking plane, where acceleration and direction changes are not easily separable. The collision avoidance pattern and the constrained behaviors in general are also inspired by studies in human sciences and psychology, leading to the concept of *personal space* (see Horowitz et al., 1964; Dosey and Meisels, 1969; Sommer, 1969). Personal space is a protective mechanism founded on the ability of the individual to perceive signals from one's physical and social environment. Its function is to create the spacing patterns that regulate distances between individuals and on which individual behaviors are based (Webb and Weber, 2003). Helbing and Molnár (1995) in their social forces model use the term "territorial effect". Several studies in psychology and sociology show how indi-

vidual characteristics influence the perception of the space and interpersonal distance. Brady and Walker (1978) found for example that anxiety states are positively correlated with interpersonal distance. Similarly, Dosey and Meisels (1969) found that individuals establish greater distances in high-stress conditions. Hartnett et al. (1974) found that male and female individuals approached short individuals more closely than tall individuals. Other studies (Phillips, 1979; Sanders, 1976) indicate that the other person's body size influences space.

2 Behavioral framework and assumptions

Individuals walk on a 2D plane and any kind of behavior influencing their movement results in two kind of observations: changes in direction and changes in speed, i.e. accelerations. This specification is important to perform walking behavior analysis, and hypotheses have to be made concerning the unobserved factors in the model and how they are related to the observed data. Figure 1 summarizes the set of assumptions we want to test. Five behavioral patterns are defined. In a discrete choice context, they have to be considered as competitive terms entering the utility functions of each alternative, as reported in Equation 1. The utilities describe the space around the decision maker and under the rational behavior assumption the individual chooses that location (alternative) with the maximum utility. In the following, we discuss the different patterns and the associated assumptions in more details.

Unconstrained patterns

The unconstrained patterns are identified by those behaviors that are independent from the presence of other pedestrians. We assume that three factors influence the individual behavior.

- **Toward destination** The first factor is represented by the choice of the final destination which can be a specific area where the individual wants to perform an activity in her schedule. To be coherent with the general framework introduced in Section 1, we assume that the destination choice is performed at the strategical level in the hierarchical decision process. Such a higher level choice is naturally reflected on the short term behavior as the tendency of individuals to choose, for the next step, a spatial location that minimize both the angular displacement and the distance to the destination.
- **Keep direction** The second factor influencing the unconstrained behavior is represented by the tendency of people to avoid frequent changings in direction. People choose their next position in order to minimize the angular displacement from their current movement direction. In addition to the behavioral motivation of this factor, it also plays a smoothing role in the model, avoiding drastic changes of direction from one time period to the next.
- **Free flow acceleration** In free flow conditions the behavior of the individual is driven by her desired speed. The acceleration is then a function of the difference between current

speed and desired speed. However, this factor is an unobserved individual characteristic and it can not be introduced explicitly in the model. As a consequence, we assume that the attractiveness of an individual for an acceleration is dependent on her current speed value. Increasing speed values correspond to decreasing attractiveness for further accelerations. A similar idea is applied to decelerations (see Antonini et al., to appear).

Constrained patterns

Constrained behaviors are induced by the presence of other individuals in the scene and capture the pedestrian-pedestrian interactions. We identify attractive and repulsive interactions, described by the following patterns.

- **Leader-follower** We assume that the decision maker is influenced by leaders. In our spatial representation 11 radial cones partition the choice set (see Figure 3). In each of these directions a possible leader can be identified among a set of *potential leaders*. A potential leader is an individual which is inside a certain region of interest, *not so far* from the decision maker and having a moving direction *close enough* to the direction of the radial cone where she is. Once identified, the leader induces an attractive interaction on the decision maker. Similarly to car following models, a leader acceleration corresponds to a decision maker acceleration.
- **Collision avoidance** This pattern captures the effects of possible collisions on the decision maker trajectory. For each direction in the choice set, a collider is identified among a set of *potential colliders*. Another individual is selected as a potential collider if she is inside a certain region of interest, *not so far* from the decision maker and walking against the decision maker herself. This pattern is associated with repulsive interactions in the obvious sense that pedestrians change their current direction to avoid collisions with other individuals.

3 The model

Following the framework proposed in Figure 1 we report here the systematic utility as perceived by individual n for the alternative identified by the speed regime v and direction d :

$$\begin{aligned}
& \left. \begin{aligned} & V_{vdn} = \beta_{dir} \mathbf{dir}_{dn} + \end{aligned} \right\} \textit{keep direction} \\
& \left. \begin{aligned} & \beta_{ddist} \mathbf{ddist}_{vdn} + \\ & \beta_{ddir} \mathbf{ddir}_{dn} + \end{aligned} \right\} \textit{toward destination} \\
& \left. \begin{aligned} & \beta_{acc} I_{v,acc} (v_n/v_{max})^{\lambda_{acc}} + \\ & \beta_{dec} I_{v,dec} (v_n/v_{max})^{\lambda_{dec}} + \end{aligned} \right\} \textit{free flow acceleration} \quad (1) \\
& \left. \begin{aligned} & I_{v,acc} I_{acc}^L \alpha_{acc}^L D_L^{\rho_{acc}^L} \Delta v_L^{\gamma_{acc}^L} \Delta \theta_L^{\delta_{acc}^L} + \\ & I_{v,dec} I_{dec}^L \alpha_{dec}^L D_L^{\rho_{dec}^L} \Delta v_L^{\gamma_{dec}^L} \Delta \theta_L^{\delta_{dec}^L} + \end{aligned} \right\} \textit{leader follower} \\
& \left. \begin{aligned} & I_{d,d_n} I_C \alpha_C e^{-\rho_C D_C} \Delta v_C^{\gamma_C} \Delta \theta_C^{\delta_C} \end{aligned} \right\} \textit{collision avoidance}
\end{aligned}$$

where all the β parameters as well as λ_{acc} , λ_{dec} , α_{acc}^L , ρ_{acc}^L , γ_{acc}^L , δ_{acc}^L , α_{dec}^L , ρ_{dec}^L , γ_{dec}^L , δ_{dec}^L , α_C , ρ_C , γ_C , δ_C are unknown and have to be estimated. Note that this specification is the result of an intensive modeling process, where many different specifications have been tested. We explain in the following the different terms of the utilities.

- **Keep direction** This behavior is captured by the term

$$\beta_{dir} \mathbf{dir}_{dn}$$

where the variable \mathbf{dir}_{dn} is defined as the angle in degrees between direction d and direction d_n , corresponding to the central cone, as shown in figure 4.

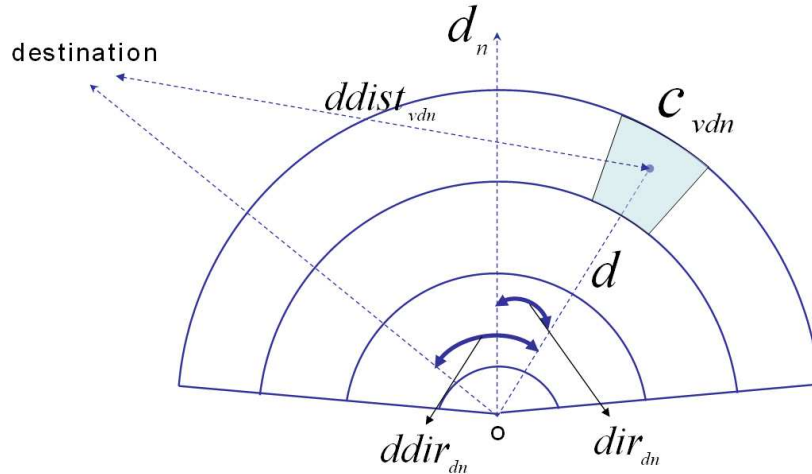


Figure 4: The elements capturing the *keep direction* and *toward destination* behaviors

- **Toward destination** This behavior is captured by the term

$$\beta_{ddist} ddist_{v_{dn}} + \beta_{ddir} ddir_{dn}$$

where the variable $ddist_{v_{dn}}$ is defined as the distance in meters between the destination and the center of the alternative $C_{v_{dn}}$, while $ddir_{dn}$ is defined as the angle in degrees between the destination and the alternative's direction d , as shown in figure 4.

- **Free flow acceleration** We define two parameters for the free flow acceleration (deceleration) terms, $\tilde{\beta}_{acc}$ and $\tilde{\beta}_{dec}$:

$$\begin{aligned}\tilde{\beta}_{acc} &= I_{v,acc} \beta_{acc} (v_n / v_{max})^{\lambda_{acc}}, \\ \tilde{\beta}_{dec} &= I_{v,dec} \beta_{dec} (v_n / v_{max})^{\lambda_{dec}}\end{aligned}$$

The attribute $I_{v,acc}$ is 1 if $v = v_{acc}$, that is, if the alternative corresponds to an acceleration and 0 otherwise. $I_{v,dec}$ is similarly defined. The two parameters are non-linear functions of the current speed of the decision-maker v_n . β_{acc} is the value of the parameter associated with $v_n = v_{max}$ and λ_{acc} is the elasticity of the parameter with respect to speed. v_{max} represents the maximum value of the observed speed module.

- **Leader-follower** The leader-follower model captures the attractive interactions among pedestrians and is given by the following terms

$$I_{v,acc} I_{acc}^L \alpha_{acc}^L D_L^{\rho_{acc}^L} \Delta v_L^{\gamma_{acc}^L} \Delta \theta_L^{\delta_{acc}^L} + I_{v,dec} I_{dec}^L \alpha_{dec}^L D_L^{\rho_{dec}^L} \Delta v_L^{\gamma_{dec}^L} \Delta \theta_L^{\delta_{dec}^L}.$$

It is described by a *sensitivity/stimulus* framework. For a given leader, the sensitivity is described by

$$sensitivity = f(D_L) = \alpha_g^L D_L^{\rho_g^L} \quad (2)$$

where D_L represents the distance between the decision maker and the leader. The parameters α_g^L and ρ_g^L have to be estimated and $g = \{acc, dec\}$ indicates when the leader is accelerating with respect to the decision maker. The decision maker reacts to stimuli coming from the chosen leader. We model the stimulus as a function of the leader's relative speed Δv_L and the leader's relative direction $\Delta \theta_L$ as follows:

$$stimulus = g(\Delta v_L, \Delta \theta_L) = \Delta v_L^{\gamma_g^L} \Delta \theta_L^{\delta_g^L} \quad (3)$$

with $\Delta v_L = |v_L - v_n|$, where v_L and v_n are the leader's speed module and the decision maker's speed module, respectively. The variable $\Delta \theta_L = \theta_L - \theta_d$, where θ_L represents

the leader's movement direction and θ_d is the angle characterizing direction d , as shown in Figure 5(a). The parameters γ_g^L and δ_g^L have to be estimated. A leader acceleration induces a decision maker's acceleration. A substantially different movement direction in the leader reduces the influence of the latter on the decision maker.

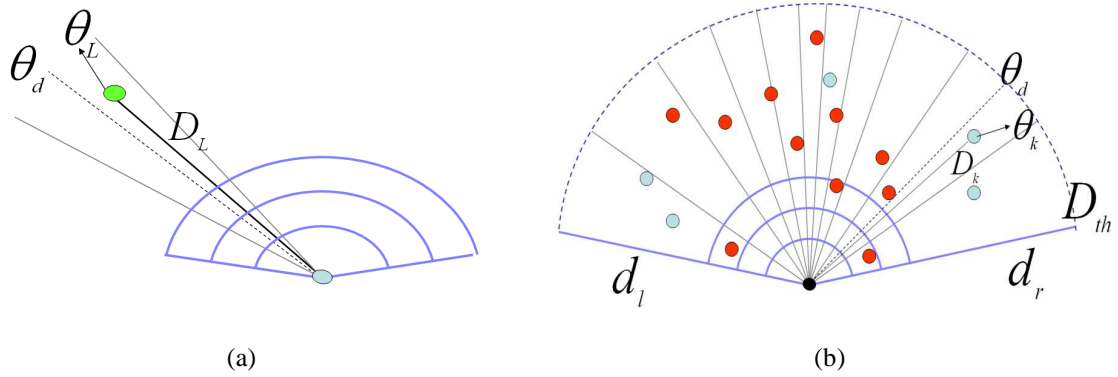


Figure 5: Figure 5(a) shows the leader's movement direction, θ_L , the direction of the radial cone where the leader lies, θ_d , and her distance from the decision maker, D_L , used in the definitions of both the sensitivity and the stimulus terms. Figure 5(b) illustrates how many potential leaders are considered for each direction and how only the nearest one is chosen as leader for a specific direction (darker circles)

The leader for each direction is chosen considering several *potential leaders*, as shown in Figure 5(b). An individual k is defined as a potential leader based on the following indicator function I_g^k :

$$I_g^k = \begin{cases} 1, & \text{if } d_l \leq d_k \leq d_r, \\ & \text{and } 0 < D_k \leq D_{th}, \\ & \text{and } 0 < |\Delta\theta_k| \leq \Delta\theta_{th} \\ 0, & \text{otherwise.} \end{cases}$$

where d_l and d_r represent the bounding left and right directions of the choice set (defining the region of interest) while d_k is the direction identifying the pedestrian k position. D_k is the distance between pedestrian k and the decision maker, $\Delta\theta_k = \theta_k - \theta_d$ is the difference between the movement direction of pedestrian k (θ_k) and the angle characterizing direction d , i.e. the direction identifying the radial cone where individual k lies (θ_d). The two thresholds D_{th} and $\Delta\theta_{th}$ are fixed at the values $D_{th} = 5D_{max}$, where D_{max} is the radius of the choice set, and $\Delta\theta_{th} = 10$ degrees. We assume an implicit *leader choice* process, executed by the decision maker herself and modelled choosing as leader for each direction the potential leader at the minimum distance $D_L = \min_{k \in K}(D_k)$, illustrated in

Figure 5(b) by the darker circles. Finally, the indicator functions $I_{v,acc}$ and $I_{v,dec}$ discriminate between accelerated and decelerated alternatives, as for the free flow acceleration model.

- **Collision avoidance** The collision avoidance model captures the repulsive interactions among pedestrians and is given by the following term

$$I_{d,d_n} I_C \alpha_C e^{-\rho_C D_C} \Delta v_C^{\gamma_C} \Delta \theta_C^{\delta_C}.$$

The scenario is similar to the leader follower. We keep the sensitivity/stimulus framework, where the sensitivity function is defined as

$$\text{sensitivity} = f(D_C) = \alpha_C e^{-\rho_C D_C} \quad (4)$$

where the parameters α_C and ρ_C have to be estimated and D_C is the distance between the collider position and the center of the alternative, as shown in Figure 6(a). We choose the exponential to keep the same functional form as that used in Antonini et al. (to appear). The decision maker reacts to stimuli coming from the collider. We model the stimulus as a function of two variables:

$$\text{stimulus} = f(\Delta v_C, \Delta \theta_C) = \Delta v_C^{\gamma_C} \Delta \theta_C^{\delta_C} \quad (5)$$

with $\Delta \theta_C = \theta_C - \theta_{d_n}$, where θ_C is the collider movement direction and θ_{d_n} is the decision maker movement direction, and $\Delta v_C = v_C + v_n$, where v_C is the collider's speed module and v_n is the decision maker's speed module. The parameters γ_C and δ_C have to be estimated. Individuals walking against the decision maker at higher speeds and in more frontal directions (higher $\Delta \theta_C$) generate stronger reactions, weighted by the sensitivity function.

The collider for each direction is chosen considering several *potential colliders*, as shown in Figure 6(b). An individual k is defined as a potential collider based on the following indicator function

$$I_C^k = \begin{cases} 1, & \text{if } d_l \leq d_k \leq d_r, \\ & \text{and } 0 < D_k \leq D'_{th}, \\ & \text{and } \frac{\pi}{2} \leq |\Delta \theta_k| \leq \pi \\ 0, & \text{otherwise.} \end{cases}$$

where d_l , d_r and d_k are the same as those defined for the leader follower model. D_k is now the distance between individual k and the center of the alternative, $\Delta \theta_k = \theta_k - \theta_{d_n}$ is the difference between the movement direction of pedestrian k (θ_k) and the movement

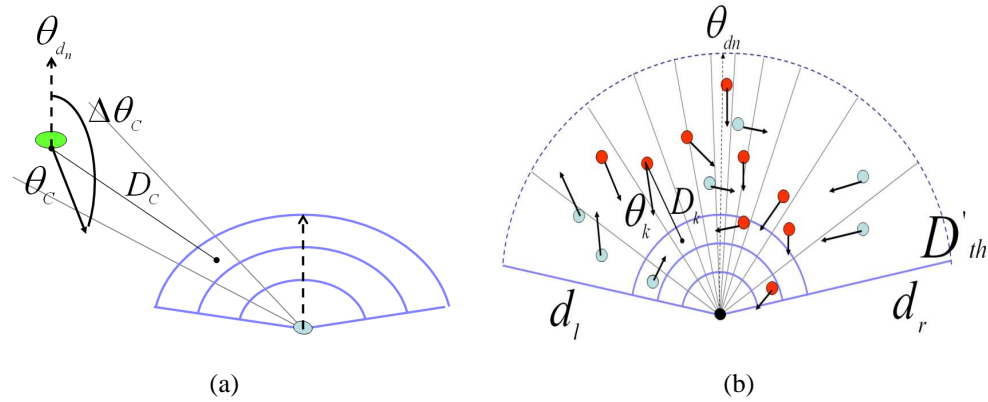


Figure 6: Figure 6(a) shows the collider and decision maker movement directions, θ_C and θ_{dn} respectively. D_C represents here the distance of the collider with the center of the alternative. Figure 6(b) shows many potential colliders taken into account for each direction

direction of the decision maker, θ_{dn} . The value of the distance threshold is now fixed to $D'_{th} = 10D_{max}$. We use a larger value for such a threshold compared to the leader-follower model, assuming the collision avoidance behavior being a longer range interaction, happening also at a lower density level. We assume an implicit *collider choice* process, executed by the decision maker herself. Among the set of K_d potential colliders for direction d , the collider is chosen as that individual having $\Delta\theta_C = \max_{k \in K_d} |\Delta\theta_k|$. The related indicator function is I_C . Finally, the collision avoidance term is included in the utility functions of all the alternatives, with the exception of the central ones. So, the indicator function I_{d,d_n} is equal to 1 for those alternatives that are not in the current direction ($d \neq d_n$), 0 otherwise.

The random term

We keep the cross nested logit (CNL) specification used in Antonini et al. (to appear). Such a model allows flexible correlation structures in the choice set, keeping a closed form solution. The CNL being a Generalized Extreme Value (GEV) model (see McFadden, 1978), the probability of choosing alternative i within the choice set C is:

$$P(i|C) = \frac{y_i G_i(y_1, \dots, y_J)}{\mu G(y_1, \dots, y_J)} \quad (6)$$

where J is the number of alternatives in C , $y_j = e^{V_j}$ with V_j the systematic part of the utility described in Section 3 and G is the following generative function:

$$G(y_1, \dots, y_J) = \sum_{m=1}^M \left(\sum_{j \in C} (\alpha_{jm}^{1/\mu} y_j)^{\mu_m} \right)^{\frac{\mu}{\mu_m}} \quad (7)$$

where M is the number of nests, $\alpha_{jm} \geq 0, \forall j, m$, $\sum_{m=1}^M \alpha_{jm} > 0, \forall j$, $\mu > 0$, $\mu_m > 0, \forall m$ and $\mu \leq \mu_m, \forall m$. This formulation leads to the following expression for the choice probability formula, using $y_i = e^{V_i}$:

$$P(i|C) = \sum_{m=1}^M \frac{\left(\sum_{j \in C} \alpha_{jm}^{\mu_m/\mu} y_j^{\mu_m} \right)^{\frac{\mu}{\mu_m}} \frac{\alpha_{im}^{\mu_m/\mu} y_i^{\mu_m}}{\sum_{j \in C} \alpha_{jm}^{\mu_m/\mu} y_j^{\mu_m}}}{\sum_{n=1}^M \left(\sum_{j \in C} \alpha_{jn}^{\mu_n/\mu} y_j^{\mu_n} \right)^{\frac{\mu}{\mu_n}}} \quad (8)$$

We assume a correlation structure depending on the speed and direction and we identify five nests: *accelerated*, *constant speed*, *decelerated*, *central* and *not central*. This correlation structure is illustrated in figure 7. Given the lack of any a priori information, we fix the degrees of membership to the different nests (α_{jm}) to the constant value 0.5.

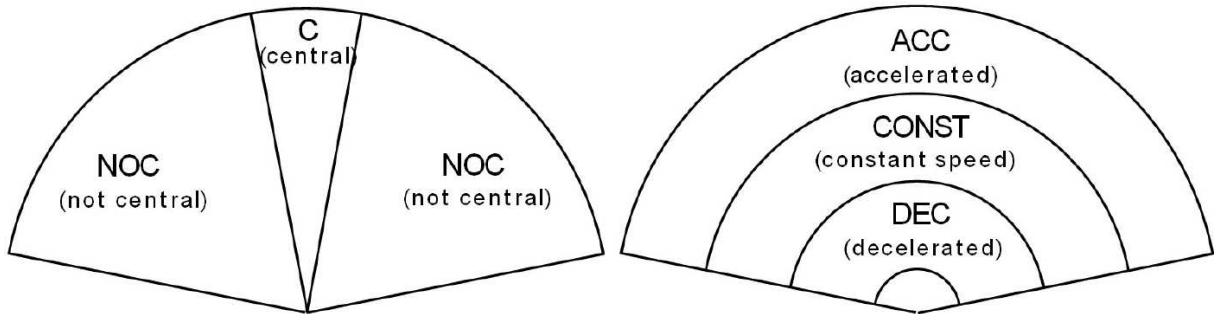


Figure 7: **left:** Nesting based on direction

right: Nesting based on speed

4 Data

The dataset used to estimate the model consists of pedestrian trajectories manually tracked from video sequences. We have pooled together two different datasets, collected separately in Switzerland and Japan.

The Swiss dataset

This part of the dataset consists of 36 pedestrian trajectories, manually tracked from a digital video sequence. The scene has been recorded out of the Flon metro station in Lausanne, in 2002, for a total of 1675 observed positions. Each position refers to a reference system on the



(a) Japanese scenario

(b) Swiss scenario

Figure 8: Images from the two scenarios used to collect the dataset.

walking plane, after a calibration of the camera. For a detailed description of this first dataset we refer the reader to Antonini et al. (to appear).

The Japanese dataset

This dataset has been collected in Sendai, Japan, on August 2000 (see Teknomo et al., 2000; Teknomo, 2002). The video sequence has been recorded from the 6th floor of the JTB parking building (around 19 meters height), situated at a large pedestrian crossing point. Two main pedestrian flows cross the street, giving rise to a large number of interactions. In this context, 190 pedestrian trajectories have been manually tracked, with a time step of 1 second, for a total number of 10200 position observations. The collected data contains the pedestrian identifier, the time step and the image coordinates. The mapping between the image plane and the walking plane is approximated by a 2D-affine transformation, whose parameters are learnt by linear regression. The reference system on the walking plane has the origin arbitrarily placed on the bottom left corner of the zebra crossing. The x axis represents the width of the crossing while the y axis is the crossing length.

Two frames from the two video sequences are reported in Figure 8. In Figure 9 we report the frequency of the revealed choices as observed in the two datasets. The three peaks in the distributions arise on the central alternatives (6, 17, 28), as expected.

We report in Figure 10 two examples of trajectories and in Figure 11(a) and Figure 11(b) the related speed-time graphs. In Figure 12 we report the speed histogram and in Table 1 the speed statistics.

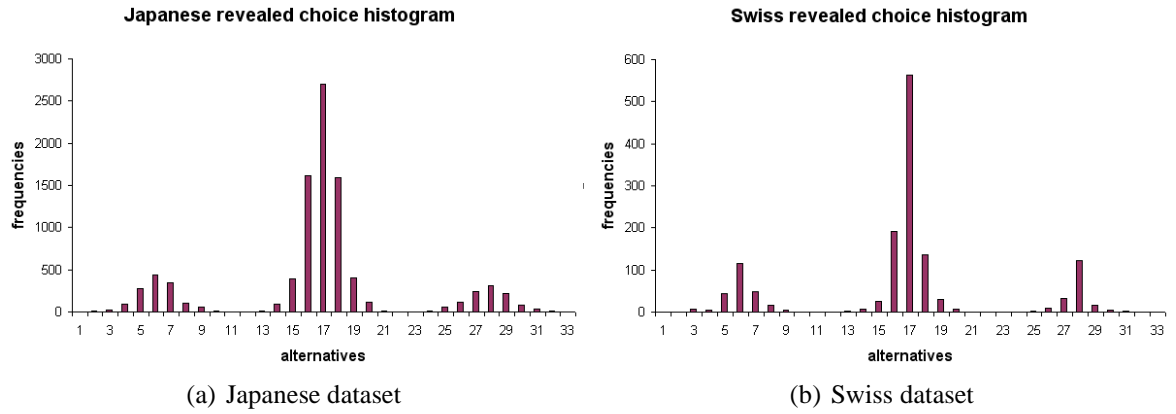


Figure 9: Revealed choices histograms.

Table 1: Speed statistics

Mean	0.668242
Standard Error	0.003547
Median	0.58023
Mode	0
Standard Deviation	0.35826
Range	3.939786
Minimum	0
Maximum	3.939786

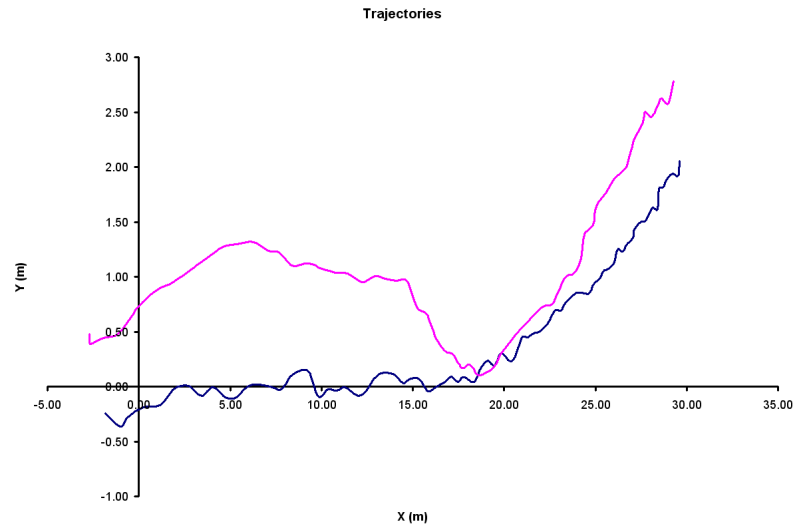


Figure 10: Examples of two manually tracked trajectories

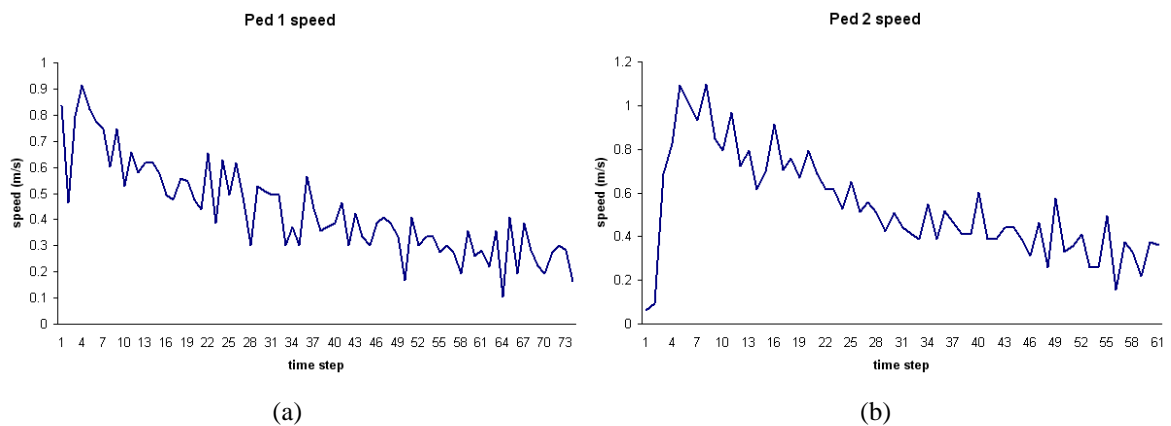


Figure 11: Speed-time graphs for the same two pedestrians

Data post-processing

The original Swiss dataset has been post-processed in order to generate the input data for the estimation process. At each step, the observed choice made by the current decision maker has been measured 3 steps ahead in time, i.e. 0.9 seconds. As a consequence, the last four positions of each trajectory are not used. Moreover, in both the datasets those observations corresponding to a static pedestrian ($v_n = 0$) and those corresponding to an observed choice out of the choice set have been discarded.

We report in Table 2 and Table 3 the averaged values of the leader and collider availabilities

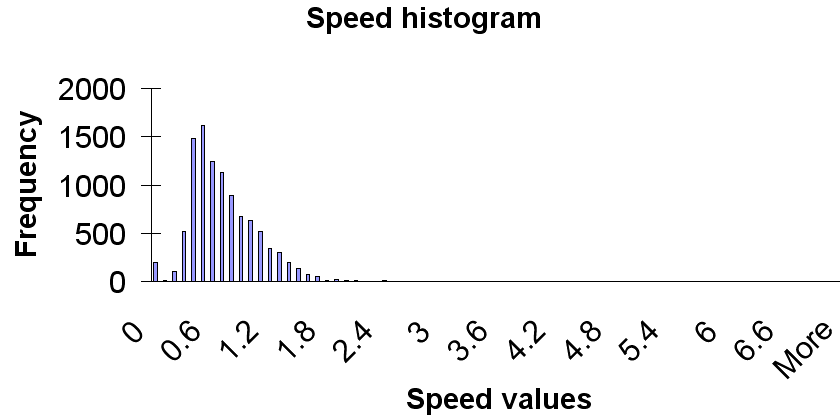


Figure 12: Speed histogram

(represented by the two indicator functions I_g^L and I_C defined above) defined as follows:

$$\begin{aligned}\bar{I}_g^L &= \frac{1}{N_S} \sum_{n=1}^{N_S} I_g^L \\ \bar{I}_C &= \frac{1}{N_J} \sum_{n=1}^{N_J} I_C\end{aligned}\quad (9)$$

where N_S and N_J are the two sample sizes.

5 Results

We report in Table 4 the estimation results. The parameters have been estimated using the Biogeme package (Bierlaire, 2003). It is a freeware package for the estimation of a wide range of random utility models.

We first shortly comment the results for those parameters related to the unconstrained models (toward destination, keep direction and free flow acceleration). This part of the model specification is similar to that presented in Antonini et al. (to appear). The *toward destination* coefficients β_{ddir} and β_{ddist} have been estimated significantly different from zero. The assumption that destination distance and direction capture two different effects is supported by the data, being related to the 2D nature of the pedestrian movements. Their signs are negative, as expected, reflecting the tendency of individuals to move directly towards their final destination, through the shortest path. The destination being exogenous to the model, we interpret this behavior as the short range projection of higher level decisions, made at the tactical level, such as (intermediate) destination choice and/or activity area choice. The *keep direction* parameter, β_{dir} , is significant and

Table 2: Averaged leader and collider availabilities for the Swiss dataset

direction	I_g^L		I_C
	accelerated	decelerated	
1	0.004	0.004	0.145
2	0.006	0.013	0.117
3	0.004	0.014	0.148
4	0.002	0.017	0.142
5	0.003	0.021	0.150
6	0.001	0.012	0.152
7	0.001	0.015	0.116
8	0.004	0.016	0.111
9	0.002	0.016	0.136
10	0.002	0.006	0.104
11	0.0007	0.002	0.069

Table 3: Averaged leader and collider availabilities for the Japanese dataset

direction	leader availability		collider availability
	accelerated	decelerated	
1	0.07	0.11	0.45
2	0.09	0.13	0.47
3	0.07	0.12	0.47
4	0.06	0.10	0.44
5	0.09	0.14	0.45
6	0.10	0.16	0.44
7	0.08	0.13	0.45
8	0.05	0.10	0.44
9	0.05	0.10	0.48
10	0.05	0.12	0.49
11	0.05	0.10	0.47

has a negative sign, as expected. It captures the tendency of people to minimize the angular displacement along their trajectories. Finally, 3 out of 4 of the *free flow acceleration* parameters, namely β_{acc} , β_{dec} and λ_{acc} have been estimated significantly different from zero. The negative signs for β_{acc} and β_{dec} indicate the tendency of pedestrians to perceive as a cost variations in speed, both positive and negative. A positive value for the acceleration elasticity λ_{acc} indicates that the attractiveness of an acceleration reduces with increases in speed, as expected.

We now comment on the constrained models' parameters. For the *leader-follower* behavior we note that in the case of an accelerated leader, 3 out of 4 parameters have been estimated significantly different from zero. The positive value for the α_{acc}^L multiplicative coefficient indicates that when a leader is present (or several potential leaders are present, so that the closest to the decision maker is considered), a leader's acceleration induces a corresponding acceleration on the decision maker. The negative sign for the distance exponential coefficient, ρ_{acc}^L , indicates that the influence of the leader on the decision maker acceleration behavior reduces when their relative distance increases, as expected. The positive sign for the speed exponential coefficient, γ_{acc}^L , shows that the utility of an acceleration increases with higher values of the relative leader speed, as expected. The same interpretation is given for the parameters corresponding to a decelerating leader. In this case we keep in the model also the exponential coefficient related to the direction, δ_{dec}^L , with t -test statistics equal to 1.642. Its negative sign is coherent with the leader-follower behavior. It reflects the fact that in those cases where the leader's relative direction is higher, the influence of the leader on the decision maker is lower, resulting in a lower utility value for the decelerated alternatives.

For the estimation of the *collision avoidance* parameters, we fix the exponential coefficient related to the collider relative direction, δ_C , equal to 1 for numerical convenience. The other three free parameters have been estimated significantly different from zero. The multiplicative coefficient α_C is negative, as expected. It indicates that those directions more likely to lead to a collision have a lower utility with respect to the central (current) direction. The latter is taken as the reference one for normalization purposes. The exponential coefficient related to the distance between the collider and the alternative, ρ_C , has a negative sign. It shows the fact that a more distant collider has a less negative impact on the alternative utility. Finally, the exponential coefficient related to the relative speed, γ_C , is positive, as expected. It captures the fact that faster colliders have a more negative impact on the utilities than slower individuals.

The correlation structure is captured by the cross nested specification. Three nest parameters have been fixed to 1 while two are left free in the model, capturing the correlation between the constant speed and the not central alternatives. They have been estimated significantly different from 1.

We finally comment on the heterogeneity in the dataset. We estimate the scale factor μ_{scale} for the Swiss data, which captures the variance of the associated error term.

We report in the following some graphics illustrating the marginal effects of the different variables for the constrained models. In Figure 13(a) and Figure 13(b) the effects of a stimulus variation (due to changes in the relative leader direction and speed) are shown. Figure 13(a) shows

an accentuated variation in the leader acceleration term which decays quite quickly when varying its relative direction. Figure 13(b) shows the acceleration term (for a fixed decision maker speed equal to 3 m/s) when the leader speed is free to vary. As expected, higher acceleration values correspond to higher relative speed values, with a zero acceleration when the leader speed is equal to the decision maker speed, as expected. In Figure 14 the effect of variations in the sensitivity function (varying the leader distance) are reported. As expected, lower acceleration terms correspond to higher relative distance values. Finally, we report in Figure 15(a), Figure 15(b) and Figure 16 an example of the probability of a central deceleration (alternative 28) when varying the relative (decelerating) leader direction, speed and distance, respectively. Similarly, in Figure 17(a) and Figure 17(b) we report the effects of variations in the stimulus term for the collision avoidance model. Figure 17(a) shows how for colliders coming from more frontal directions with respect to the decision maker direction (increasing relative direction), the collision term is reduced, reducing the alternative's utility. Figure 17(b) shows how the collision term reduces for higher relative collider speed values. In Figure 18 the effects of changes in the sensitivity term are reported. It shows how farther colliders induced a lower negative effect on the utility, i.e. the collision term increases. Finally, we report in Figure 19(a), Figure 19(b) and Figure 20 an example of the probability of a central acceleration (alternative 6) when varying the relative collider direction, speed and distance, respectively.

We conclude this section underlying the fact that it seems natural that individual characteristics such as age, sex, weight, height among others influence the spatial perception, interpersonal distance and human-human interactions. However, given the available data (trajectories) it is not possible to take into account such characteristics. The setting of controlled experimental conditions (Hoogendoorn (in press) and Daamen (2004)) is necessary to allow for such unobserved heterogeneity to be taken into account.

6 Conclusions

In this paper we propose a general framework based on discrete choice modeling for pedestrian walking behavior. The short range walking behavior of individuals is modeled, identifying two main patterns: constrained and unconstrained. The main contribution of this paper is on the former. The constraints are generated by the interactions with other individuals. We identify attractive and repulsive interactions, captured respectively through a leader-follower and a collision avoidance models. Inspiration is taken from driver behaviors in transportation science, and ideas such as the car following model and lane changing models have been reviewed and re-adapted to the more complex pedestrian case. The difficulties to collect pedestrian data as well as the limited information conveyed by pure dynamic datasets limit the possibilities in the model specification step. Important individual effects cannot be captured without the support of socio-economic characteristics. However, the recent development of pedestrian laboratories, where the set up of controlled experimental conditions is possible, represents an important step in this direction. In this spirit, important future research can be done, integrating for example

the spatial layout as an important cause for pedestrian movements as well as latent variable models capturing the effect of individual characteristics.

Acknowledgment

This work is supported by the Swiss National Science Foundation under the NCCR-IM2 project.

References

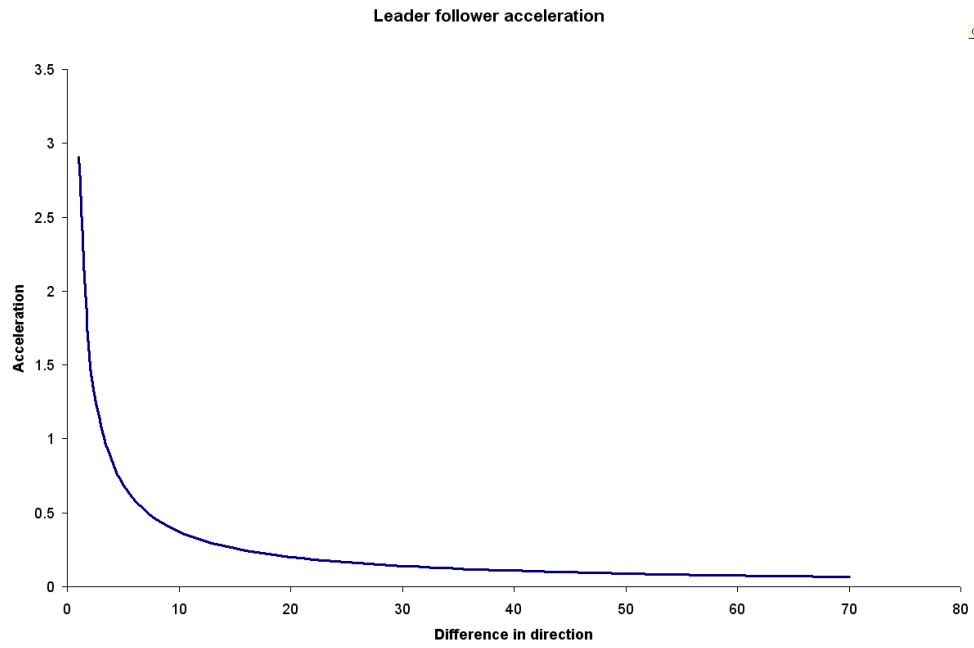
- Ahmed, K. I., 1999. Modeling drivers' acceleration and lane changing behaviors. Ph.D. thesis, Massachusetts Institute of Technology, Cambridge, MA.
- Antonini, G., Bierlaire, M., Weber, M., to appear. Discrete choice models of pedestrian walking behavior. *Transportation Research Part B* Accepted for publication.
- Bierlaire, M., 2003. BIOGEME: a free package for the estimation of discrete choice models. In: *Proceedings of the 3rd Swiss Transportation Research Conference*. Ascona, Switzerland, www.strc.ch.
- Bierlaire, M., Antonini, G., Weber, M., 2003. Behavioral dynamics for pedestrians. In: Axhausen, K. (Ed.), *Moving through nets: the physical and social dimensions of travel*. Elsevier, pp. 1–18.
- Blue, V. J., Adler, J. L., March 2001. Cellular automata microsimulation for modeling bi-directional pedestrian walkways. *Transportation Research Part B* 35 (3), 293–312.
- Borgers, A., Timmermans, H., April 1986. A model of pedestrian route choice and demand for retail facilities within inner-city shopping areas. *Geographical analysis* 18 (2), 115–128.
- Brady, A. T., Walker, M. B., 1978. Interpersonal distance as a function of situationally induced anxiety. *British Journal of Social and Clinical Psychology* 17, 127–133.
- Daamen, W., 2004. Modelling passenger flows in public transport facilities. Ph.D. thesis, Delft University of Technology, Delft, The Netherlands, the Netherlands TRAIL research school.
- Dellaert, B. G., Arentze, T. A., Bierlaire, M., Borgers, A. W., Timmermans, H. J., may 1998. Investigating consumers' tendency to combine multiple shopping purposes and destinations. *Journal of Marketing Research* 35 (2), 177–188.
- Dosey, M. A., Meisels, M., 1969. Personal space and self-protection. *Journal of Personality and Social Psychology* 11 (2), 93–97.

- Hartnett, J. J., Bailey, K. G., Hartley, C. S., 1974. Body height, position, and sex as determinants of personal space. *Journal of Psychology* 87, 129–136.
- Helbing, D., Farkas, I., Molnar, P., Vicsek, T., 2002. Simulation of pedestrian crowds in normal and evacuation simulations. In: Schreckenberg, M., Sharma, S. (Eds.), *Pedestrian and Evacuation Dynamics*. Springer, pp. 21–58.
- Helbing, D., Molnár, P., 1995. Social force model for pedestrian dynamics. *Physical review E* 51 (5), 4282–4286.
- Herman, R., Rothery, R. W., 1965. Car following and steady-state flow. In: Almond, J. (Ed.), *Proceedings on 2nd International Symposium on Theory of Traffic Flow*. O.E.C.D., Paris, France, pp. 1–11.
- Hoogendoorn, S., in press. Pedestrian travel behavior modeling. In: Axhausen, K. (Ed.), *Moving through nets: the physical and social dimensions of travel*. Elsevier, Lucerne.
- Horowitz, J. J., Duff, D. F., Stratton, L. O., 1964. Body buffer zone: Exploration of personal space. *Archives of General Psychiatry* 11 (6), 651–656.
- Lee, G., 1966. A generalization of linear car following theory. *Operations Research* 14, 595–606.
- McFadden, D., 1978. Modelling the choice of residential location. In: A. Karlquist *et al.* (Ed.), *Spatial interaction theory and residential location*. North-Holland, Amsterdam, pp. 75–96.
- Newell, G., 1961. Nonlinear effects in the dynamics of car following. *Operations Research* 9, 209–229.
- Penn, A., Turner, A., 2002. Space syntax based agent simulation. In: Schreckenberg, M., Sharma, S. (Eds.), *Pedestrian and Evacuation Dynamics*. Springer, pp. 99–114.
- Phillips, J. R., 1979. An exploration of perception of body boundary, personal space, and body size in elderly persons. *Perceptual and Motor Skills* 48, 299–308.
- Sanders, J. L., 1976. Relationship of personal space to body image boundary definiteness. *Journal of Research in Personality* 10, 478–481.
- Schadschneider, A., 2002. Cellular automaton approach to pedestrian dynamics — Theory. In: Schreckenberg, M., Sharma, S. (Eds.), *Pedestrian and Evacuation Dynamics*. Springer, pp. 75–86.
- Sommer, R., 1969. *Personal Space: The behavioral bases of design*. Prentice Hall, Englewood Cliffs, NJ.

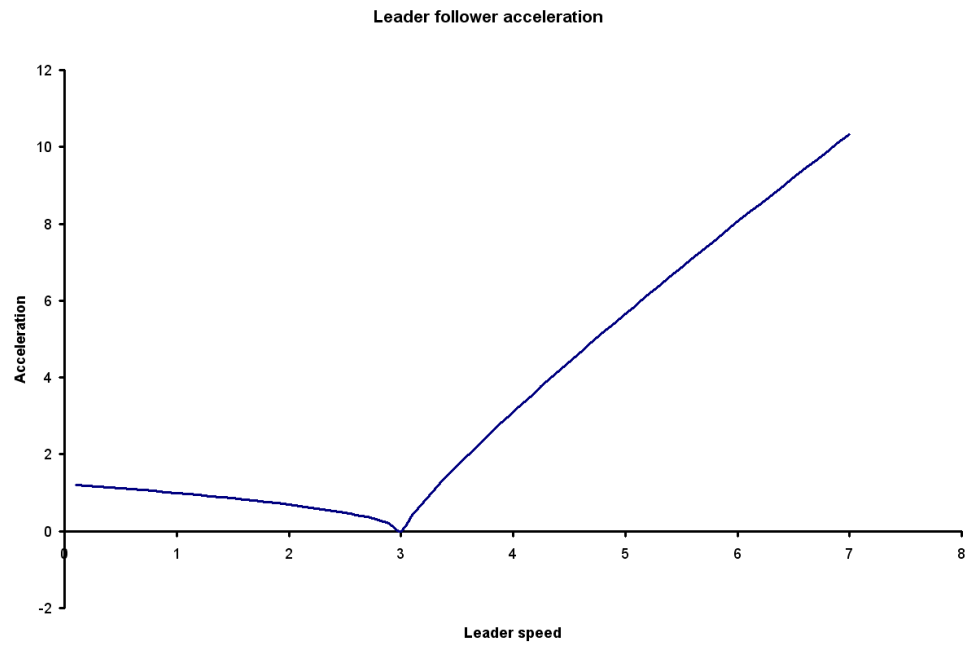
- Teknomo, K., 2002. Microscopic pedestrian flow characteristics: Development of an image processing data collection and simulation model. Ph.D. thesis, Tohoku University, Japan, Sendai.
- Teknomo, K., Takeyama, Y., Inamura, H., 2000. Review on microscopic pedestrian simulation model. In: Proceedings Japan Society of Civil Engineering Conference. Morioka, Japan.
- Toledo, T., 2003. Integrated driving behavior modeling. Ph.D. thesis, Massachusetts Institute of Technology, Cambridge, MA.
- Turner, A., 2001. Angular analysis. In: Peponis, J., Wineman, J., Bafna, S. (Eds.), Proceedings 3rd International Symposium on Space Syntax. pp. 30.1–30.11.
- Webb, J. D., Weber, M. J., September 2003. Influence of sensor abilities on the interpersonal distance of the elderly. *Environment and behavior* 35 (5), 695–711.
- Whynes, D., Reedand, G., Newbold, P., 1996. General practitioners' choice of referral destination: A probit analysis. *Managerial and Decision Economics* 17 (6), 587.

Table 4: CNL estimation results for the pooled dataset

Variable name	Coefficient estimate	t test 0	t test 1
β_{dir}	-0.061	-19.066	
β_{dist}	-1.614	-1.9749	
β_{dir}	-0.027	-11.342	
β_{acc}	-19.822	-5.847	
β_{dec}	-2.069	-2.651	
λ_{acc}	0.969	26.880	
α_{acc}^L	4.883	3.368	
ρ_{acc}^L	-0.657	-3.034	
γ_{acc}^L	0.869	9.877	
α_{dec}^L	4.061	6.278	
ρ_{dec}^L	-0.481	-4.280	
γ_{dec}^L	0.524	9.089	
δ_{dec}^L	-0.892	-1.642	
α_C	-0.0058	-4.639	
ρ_C	-0.313	6.748	
γ_C	0.781	3.318	
μ_{const}	1.597	32.413	12.119
$\mu_{not_central}$	1.487	15.765	5.160
μ_{scale}	0.591	-	-8.565
Sample size = 10783			
Number of estimated parameters = 19			
Init log-likelihood = -78558.3			
Final log-likelihood = -22572.7			
Likelihood ratio test = 30260.3			
$\bar{\rho}^2 = 0.4007$			



(a) Marginal effect of the relative leader direction



(b) Marginal effect of the relative leader speed

Figure 13: Effects of variations in the leader stimulus parameters

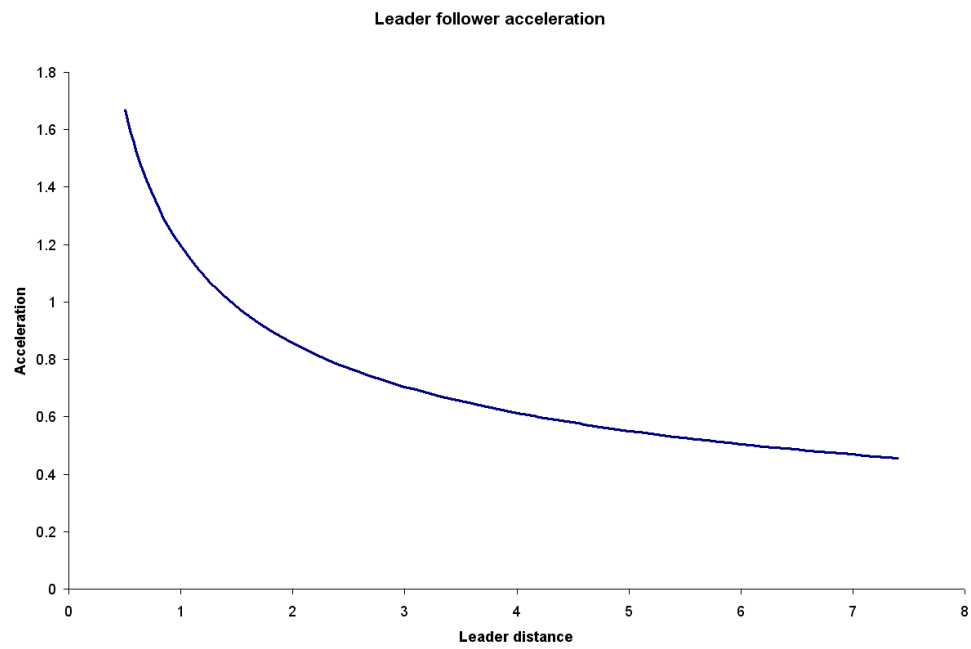
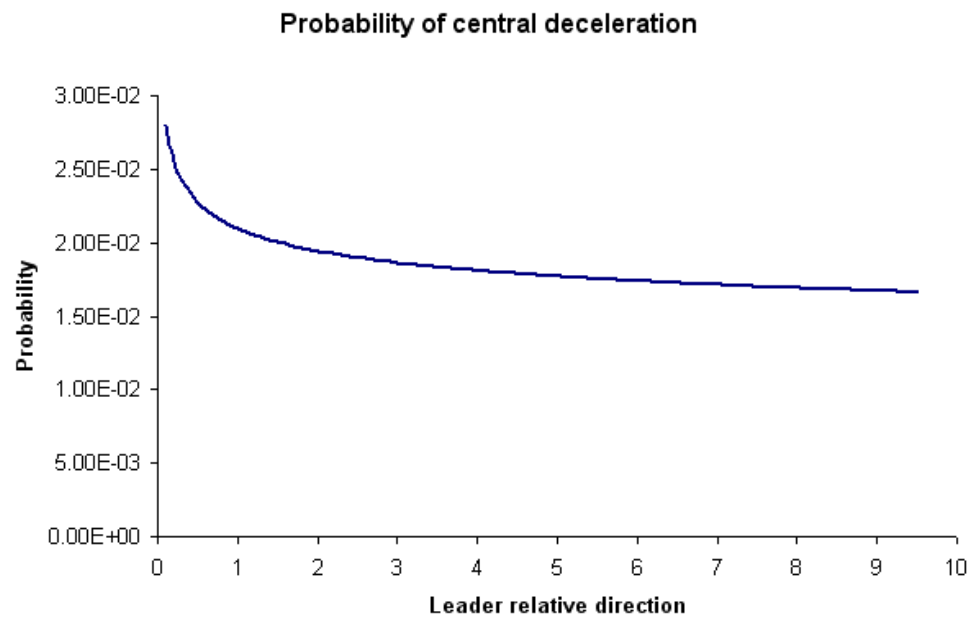
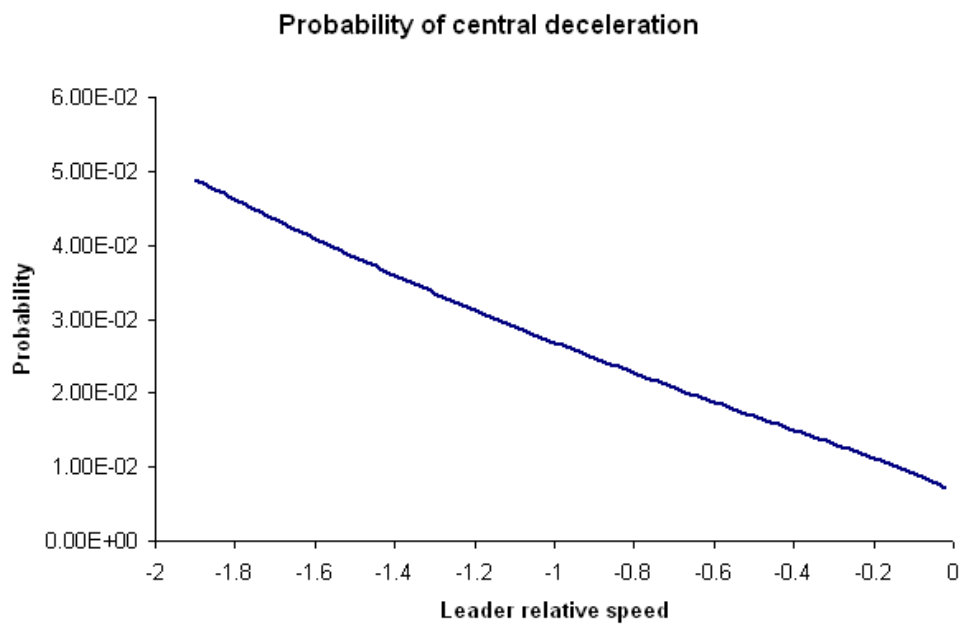


Figure 14: Effects of variations in the leader sensitivity



(a) Probability of central deceleration as a function of the relative (decelerating) leader direction



(b) Probability of central deceleration as a function of the relative (decelerating) leader speed

Figure 15: Variations in probability as a function of the leader parameters

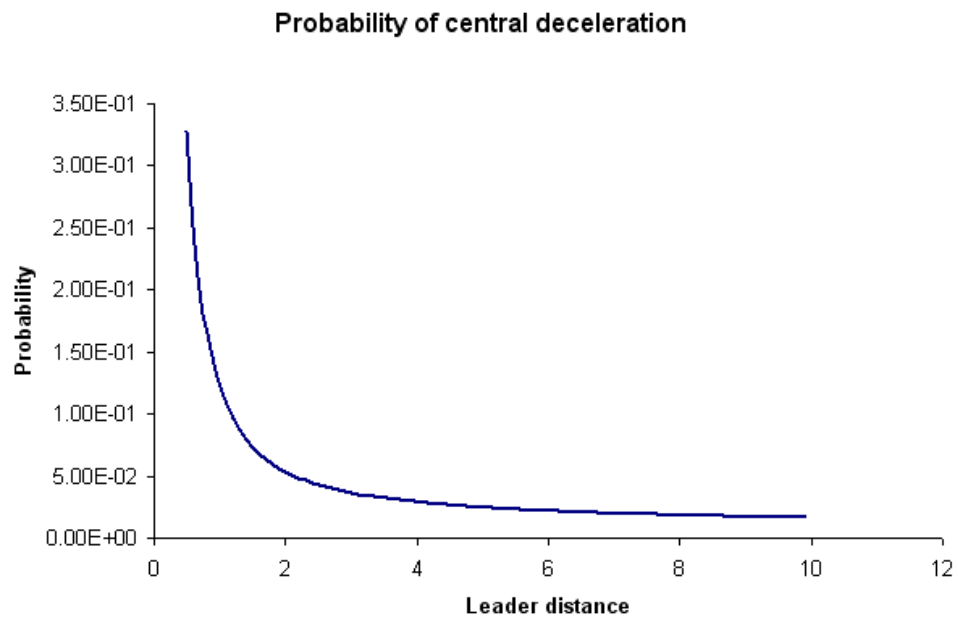
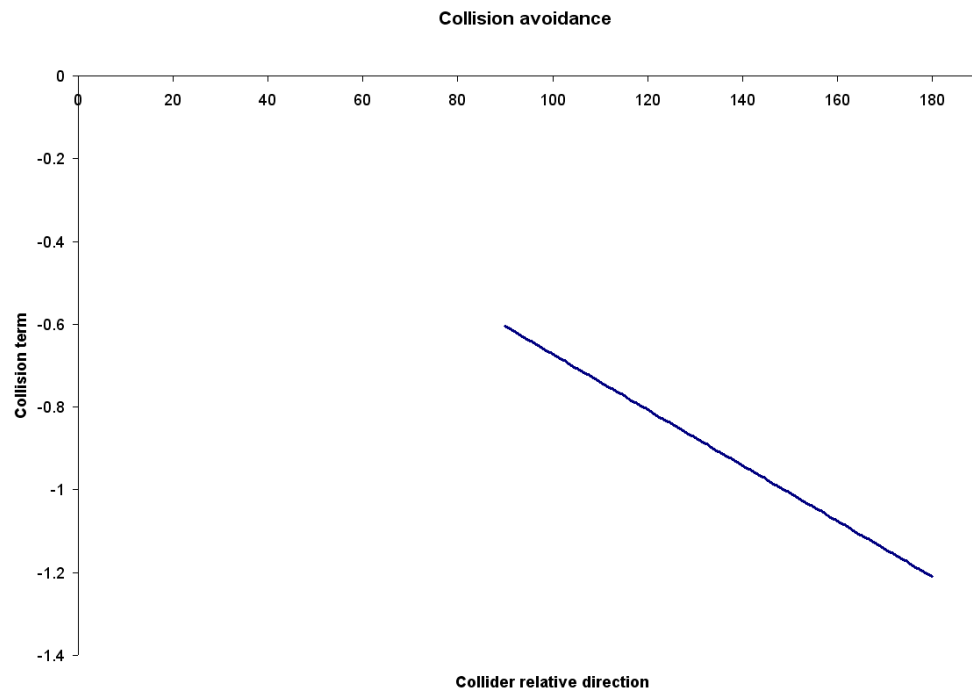
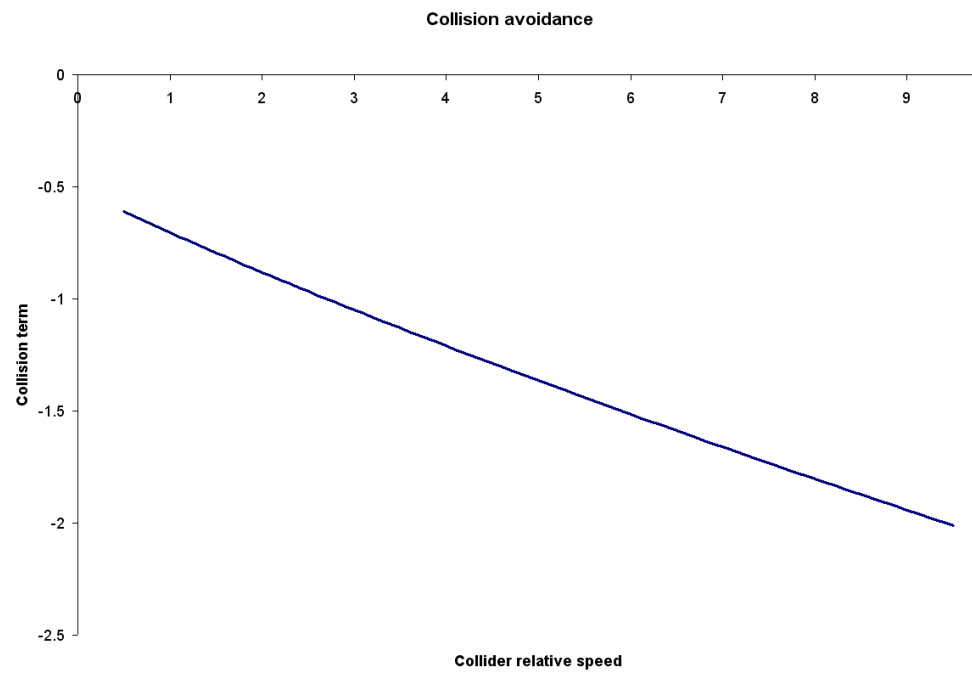


Figure 16: Probability of central deceleration as a function of the relative (decelerating) leader distance



(a) Marginal effect of the relative collider direction



(b) Marginal effect of the relative collider speed

Figure 17: Effects of variations in the collider stimulus parameters

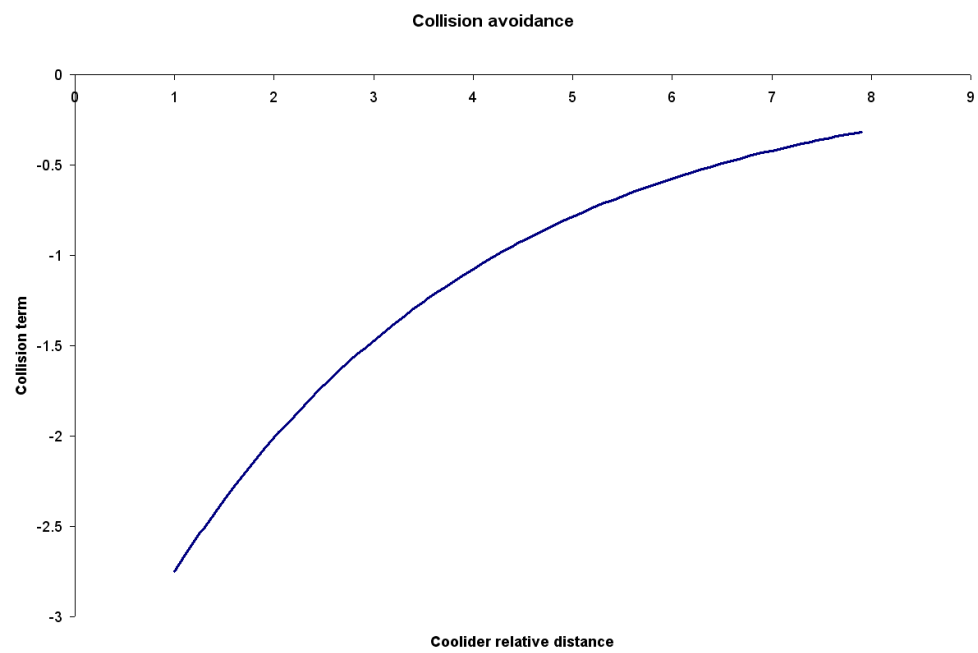
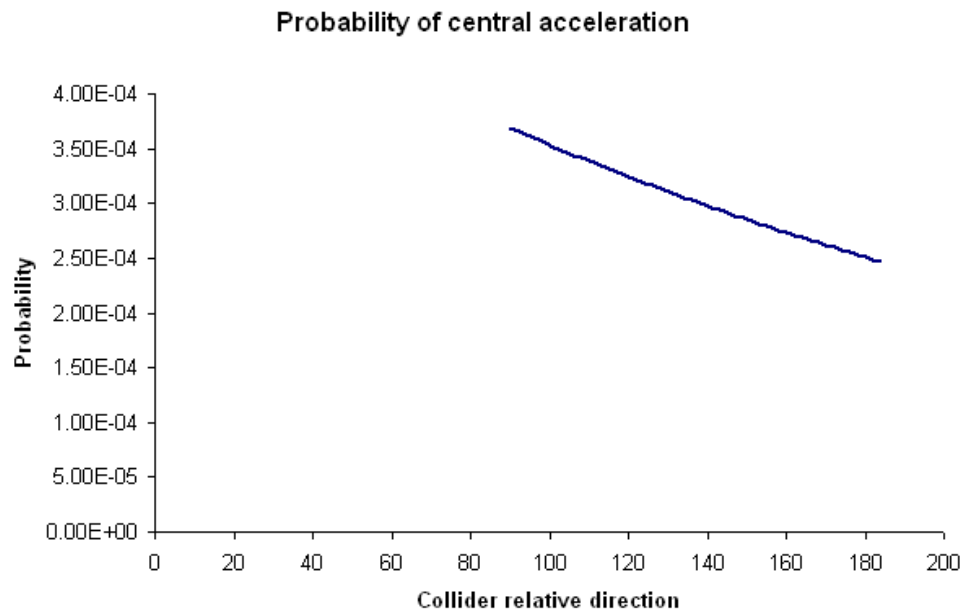
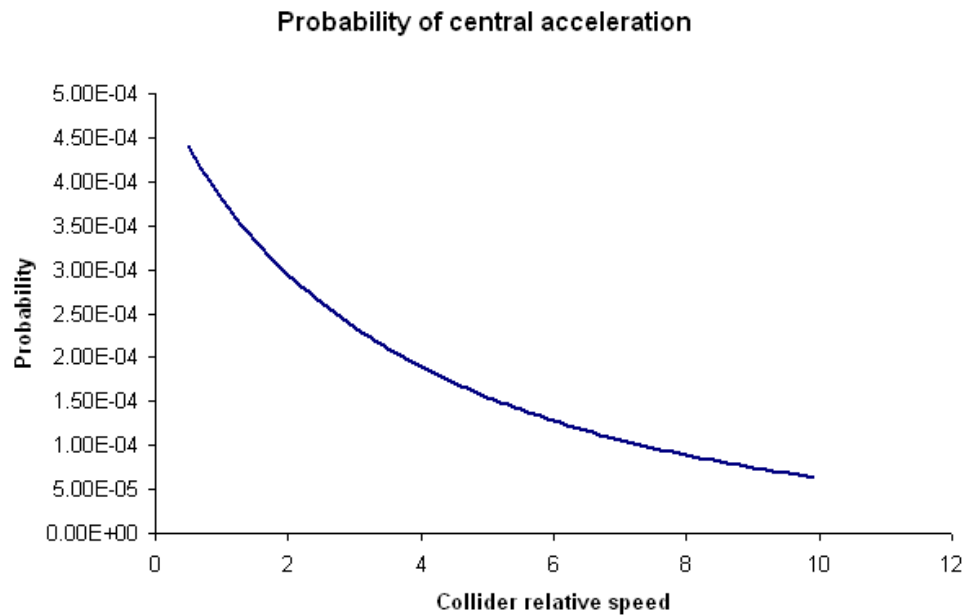


Figure 18: Effects of variations in the collider sensitivity



(a) Probability of central acceleration as a function of the relative collider direction



(b) Probability of central acceleration as a function of the relative collider speed

Figure 19: Variations in probability as a function of the collider parameters

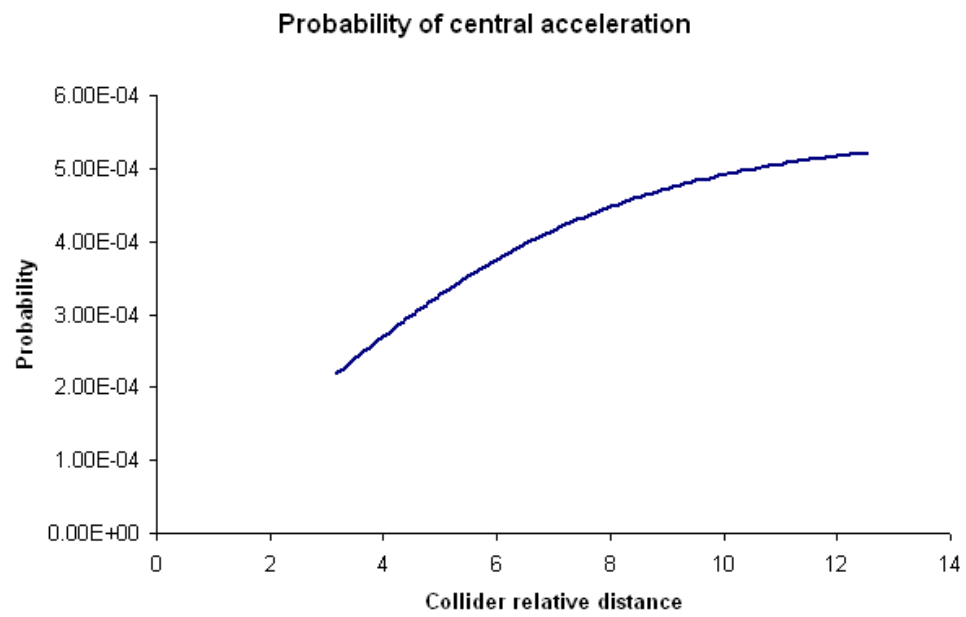


Figure 20: Probability of central acceleration as a function of the relative collider distance